

Journal Pre-proof

Use of an NIR MEMS spectrophotometer and visible/NIR hyperspectral imaging systems to predict quality parameters of treated ground peppercorns

Carlos A. Esquerre, Eva M. Achata, Marco García-Vaquero, Zhihang Zhang, Brijesh Tiwari, Colm P. O'Donnell



PII: S0023-6438(20)30750-7

DOI: <https://doi.org/10.1016/j.lwt.2020.109761>

Reference: YFSTL 109761

To appear in: *LWT - Food Science and Technology*

Received Date: 11 March 2020

Revised Date: 15 May 2020

Accepted Date: 14 June 2020

Please cite this article as: Esquerre, C.A., Achata, E.M., García-Vaquero, M., Zhang, Z., Tiwari, B., O'Donnell, C.P., Use of an NIR MEMS spectrophotometer and visible/NIR hyperspectral imaging systems to predict quality parameters of treated ground peppercorns, *LWT - Food Science and Technology* (2020), doi: <https://doi.org/10.1016/j.lwt.2020.109761>.

This is a PDF file of an article that has undergone enhancements after acceptance, such as the addition of a cover page and metadata, and formatting for readability, but it is not yet the definitive version of record. This version will undergo additional copyediting, typesetting and review before it is published in its final form, but we are providing this version to give early visibility of the article. Please note that, during the production process, errors may be discovered which could affect the content, and all legal disclaimers that apply to the journal pertain.

© 2020 Published by Elsevier Ltd.

CRedit author statement

Carlos A. Esquerre: Conceptualization, Methodology, Software, Formal analysis, Writing - Original Draft and Writing - Review & Editing, **Eva M. Achata:** Investigation and Data Curation, **Marco García-Vaquero:** Conceptualization, Methodology and Investigation, **Zhihang Zhang:** Investigation and Data Curation **Brijesh Tiwari:** Conceptualization, Methodology and Supervision, **Colm P. O'Donnell:** Conceptualization, Methodology, Writing - Review & Editing and Supervision

Journal Pre-proof

1 **Use of an NIR MEMS spectrophotometer and visible/NIR hyperspectral imaging**
2 **systems to predict quality parameters of treated ground peppercorns**

3 Carlos A. Esquerre^a, Eva M. Achata^a, Marco García-Vaquero^b, Zhihang Zhang^c, Brijesh
4 Tiwari^c, Colm P. O'Donnell^a

5 ^a School of Biosystems and Food Engineering, College of Engineering and Architecture,
6 University College Dublin, Dublin, D04V1W8, Ireland.

7 ^b School of Agriculture and Food Science, College of Health and Agricultural Sciences,
8 University College Dublin, Dublin, D04V1W8, Ireland.

9 ^c Department of Food Chemistry and Technology, Teagasc Food Research Centre, Ashtown,
10 Dublin, D15KN3K, Ireland.

11

12 **Abstract**

13 The aim of this study was to investigate the potential of a micro-electromechanical NIR
14 spectrophotometer (NIR-MEMS) and visible (Vis)/NIR hyperspectral imaging (HSI) systems
15 to predict the moisture content, antioxidant capacity (DPPH, FRAP) and total phenolic
16 content (TPC) of treated ground peppercorns. Partial least squares (PLS) models were
17 developed using spectra from peppercorns treated with hot-air, microwave and cold plasma.
18 The spectra were acquired using three spectroscopy systems: NIR-MEMS (1350 – 1650 nm),
19 Vis-NIR HSI (450-950 nm) and NIR HSI (957-1664 nm). Very good predictions of TPC
20 (RPD > 3.6) were achieved using NIR-MEMS. The performance of models developed using
21 Vis-NIR HSI and NIR HSI were good or very good for DPPH (RPD > 3.0), FRAP (RPD
22 >2.9) and TPC (RPD > 3.8). This study demonstrated the potential of NIR-MEMS and Vis-
23 NIR/NIR HSI to predict the moisture content, antioxidant capacity and total phenolic content

24 of peppercorns. The spectroscopy technologies investigated are suitable for use as in-line
25 PAT tools to facilitate improved process control and understanding during peppercorn
26 processing.

Journal Pre-proof

27 1. Introduction

28 Pepper (*Piper nigrum* L.) is a widely used spice (Meghwal & Goswami, 2013; Shityakov et
29 al., 2019). Black, green and white peppercorns are obtained from the same plant species but
30 differ in the manner of preparation for the market, resulting in different flavours and degrees
31 of spiciness (Nikolić et al., 2015). Black peppercorns are prepared by briefly cooking and
32 drying the unripe corns, white peppercorns consist of the dried ripe corns with the outer
33 pericarp removed, while green peppercorns are harvested unripe and then dried (Friedman et
34 al., 2008; Meghwal & Goswami, 2013). The *Piper nigrum* L. plant is rich in essential oil (2–3
35 %) and is a source of numerous biologically active constituents such as monoterpenes,
36 sesquiterpenes, and other volatile compounds (Nikolić et al., 2015). Piperine is the major
37 pungent alkaloid present in the corns of *Piper nigrum* L. and is associated with
38 immunomodulatory, anti-oxidant, anti-asthmatic, anti-carcinogenic, anti-inflammatory, anti-
39 ulcer, anti-amoebic (Meghwal & Goswami, 2013) and diuretic properties (Shityakov et al.,
40 2019). Pink peppercorns (*Schinus terebinthifolius*) are used as condiments and have a high
41 demand in the spice market. Extracts rich in phenolic substances from the residues of the pink
42 pepper tree processing industry exhibited significant activity against multidrug-resistant
43 bacteria (Gomes et al., 2020).

44 Preservation of peppercorns may be achieved by application of several process treatments
45 which reduce the moisture content and/or improve microbial quality. Hot air drying is the
46 most widely employed processing treatment for peppercorns. Recent studies have proposed
47 the use of microwave assisted drying and cold plasma (Charoux et al., 2020) for peppercorn
48 processing. Peppercorns treated with microwaves had improved retention of the main aroma
49 compounds (Plessi, Bertelli, & Miglietta, 2002). The use of microwaves combined with hot
50 air drying increases the efficiency of the drying process, improves moisture uniformity,
51 shortens the drying time while reducing thermal effects on bioactives (Schiffmann, 2014).

52 Cold plasma is a non-thermal technology that has been used as an alternative for microbial
53 inactivation in solid and liquid foods (Charoux et al., 2020; Misra et al., 2014). Montenegro,
54 Ruan, Ma, and Chen (2002) reported that cold plasma discharges applied directly to the food
55 product proved effective in reducing the number of *Escherichia coli* O157:H7 cells in apple
56 juice, by up to 7 log units.

57 Quality and process control measurements in the food industry are frequently carried out off-
58 line in laboratories rather than on-line. The resultant delay incurred between sampling and
59 measurement limits optimisation and control of production processes. Adoption of in-line
60 process analytical technology (PAT) tools leads to an improved understanding of both the
61 process and product variability (O'Donnell, Fagan, & Cullen, 2014). This enhanced
62 understanding enables efficient process control strategies and real-time process feedback, as
63 well as continuous knowledge building of the process itself (O'Donnell et al., 2014). Potential
64 benefits of PAT adoption are considerable and include higher quality products, improved
65 product consistency and reduced manufacturing costs (Pu, O'Donnell, Tobin, & O'Shea,
66 2020). Visible (Vis)/NIR spectroscopy is one of the most promising sensing approaches for
67 in-line control of peppercorns preservation processing (Lapcharoensuk et al., 2019; Orrillo et
68 al., 2019; Wilde, Haughey, Galvin-King, & Elliott, 2019). The advantages of spectroscopic
69 methods for bioprocess monitoring are manifold and include real-time capability, non-
70 destructive nature, ease of maintenance and the possibility for simultaneous determination of
71 multiple target analytes (Zimmerleiter et al., 2019). NIR combined with multivariate data
72 analysis has been previously used for rapid determination of piperine and other pepper oil
73 components in black and white ground pepper (Schulz, Baranska, Quilitzsch, Schütze, &
74 Lösing, 2005), and to detect adulteration of ground black pepper (Wilde et al., 2019).
75 Challenges to the adoption of Vis-NIR spectroscopy for in-line process control applications

76 include PAT tool robustness in a plant environment, limited field of view and the
77 development of the chemometric models required.

78 Advances in microelectromechanical systems (MEMS), semiconductors, computing
79 capabilities, and chemometrics have allowed the miniaturisation of systems for field and
80 inline applications (Rodriguez-Saona & Aykas, 2019). MEMS transducers are fabricated
81 using solid-state micromachining techniques commonly used by the semiconductor industry
82 in the production of integrated circuits (Mendelson, 2012). Miniature spectrophotometers
83 which use MEMS technology are compact, robust and relatively low cost devices
84 (Zimmerleiter et al., 2019). MEMS-based Fabry-Perot interferometers have been employed in
85 miniaturised NIR spectrophotometers (Yan & Siesler, 2018). The use of common optical
86 paths in Fabry-Perot interferometers (FPI) make them less sensitive to environmental
87 disturbances than Michelson interferometers which use different optical paths (Wang, Shyu,
88 & Chang, 2010). MEMS based FPI usually consist of a vertically integrated structure
89 composed of two mirrors separated by an air gap, wavelength tuning is achieved by applying
90 the voltage between the two mirrors resulting in an electrostatic force which pulls the mirror
91 closer. However the main disadvantage associated with two mirrors FPI is limited spectral
92 range (Parashar, Shah, Packirisamy, & Sivakumar, 2007).

93 Hyperspectral imaging also known as chemical or spectroscopic imaging, is a PAT tool for
94 food quality and safety control that integrates conventional imaging and spectroscopy to
95 obtain both spatial and spectral information from a sample (Gowen, O'Donnell, Cullen,
96 Downey, & Frias, 2007). Use of hyperspectral imaging systems facilitate improved
97 inspection of raw material, in-process and final product. Hyperspectral images or hypercubes
98 consist of several congruent images representing intensities at different spectral bands and
99 spatial positions. These hypercubes are three-dimensional blocks of data, comprising one
100 spectral (λ) and two spatial dimensions (X, Y). Each pixel in a hyperspectral image contains

101 the spectrum of that specific position, representing the light-absorbing and/or scattering
102 properties of the spatial region represented, which can be used to characterise the
103 composition of that particular pixel (Gowen et al., 2007). NIR-HSI has been evaluated for
104 prediction of black pepper adulteration with papaya seeds (Orrillo et al., 2019) and to identify
105 samples treated with selected preservation technologies (Achata, Inguglia, Esquerre, Tiwari,
106 & O'Donnell, 2019).

107 Principal component analysis (PCA) is frequently employed as an exploratory tool in
108 chemometric analysis of Vis-NIR spectral data. PCA transforms a spectral dataset with highly
109 correlated spectral bands into a smaller set of uncorrelated components. This reduces the
110 original dataset, filtering noise and redundancies based on the variance–covariance structure
111 of the original data, to reveal hidden and simplified structure/patterns (Mujica, Rodellar,
112 Fernández, & Güemes, 2010). Partial least squares (PLS) is the most commonly used
113 regression method to predict composition or quality parameters using Vis-NIR spectroscopy
114 data. Spectral pre-treatments may be employed to correct for the effects of light scattering
115 and differences in the effective path length on Vis-NIR spectra and improve the performance
116 of PLS models (Esquerre, Gowen, Burger, Downey, & O'Donnell, 2012). Variable selection
117 methods have also improved the performance of Vis-NIR PLS models and reduced the
118 processing times required by selecting the most informative wavelengths (Achata et al.,
119 2019).

120 The aim of this study was to investigate the use of an NIR MEMS spectrophotometer and
121 Vis-NIR/NIR hyperspectral imaging systems to predict the moisture content, antioxidant
122 capacity and total phenolic content of treated ground peppercorns.

123

124 **2. Materials and methods**

125 **2.1. Peppercorn samples**

126 Black, white and green (*Piper nigrum*) and pink peppercorns (*Schinus terebinthifolius*) were
127 used in this study. Black peppercorns produced in India were purchased from East End Foods
128 PLC (West Bromwich, UK). White, green and pink peppercorns were purchased from
129 Greenfields (London, UK). All the samples were ground using a blender mill (Cookworks,
130 China) and sieved to 1 mm particle size using a sieve-shaker (VWR International LLC,
131 Ireland). Ground peppercorn samples of each type (i.e. black, white, green and pink peppers)
132 were grouped into 41 subsamples of 5 g each for treatment as described in section 2.2 ($n = 4$
133 peppercorn types \times 41 subsamples = 164).

134

135 **2.2. Process treatments of ground peppercorns**

136 The following treatments were applied to the ground peppercorns samples: (1) hot air drying
137 (Drying chamber E28, Binder, Germany) at selected temperatures (40, 60, 80 or 100 °C) and
138 treatment times (5, 10, 15 and 20 min) ($n = 4$ temperatures \times 4 times \times 4 peppercorn types =
139 64); (2) microwave oven-drying (NN-CF778S, Panasonic, UK) at selected power levels (250,
140 400, 600 or 1000 W) and treatment times (1, 2, 3 and 5 min) ($n = 4$ power levels \times 4 times \times
141 4 peppercorn types = 64); and (3) cold plasma treatment (Leap100, PlasmaLeap
142 Technologies, Ireland) at selected voltages (150 and 300 V) and treatment times (5, 10, 15
143 and 20 min) ($n = 2$ voltage \times 4 time \times 4 peppercorn type = 32). Treated ($n = 160$) and control
144 samples ($n = 4$) were placed in a desiccator for 20 min, packed and stored in dark conditions
145 prior to analyses. Treated and control samples' spectra were acquired as described in section
146 2.4. Each sample was split for moisture analysis (1 g) and for antioxidant capacity and total
147 phenolic analyses (2 g, Section 2.3). Moisture content was determined by oven-drying the
148 samples at 105 °C for 16 h.

149 **2.3. Antioxidant capacity and total phenolic content analyses**

150 All ground peppercorn samples (n= 164) were further processed for antioxidant capacity and
151 total phenolic content analyses. Briefly, ground peppercorn samples were mixed thoroughly
152 with an 80 % methanolic solution (1:10, w/v) and placed in an orbital shaker (Heildolph
153 instruments, Schwabach, Germany) at 170 rpm at room temperature overnight. The extracts
154 were filtrated, evaporated, freeze-dried and stored at -20 °C before further analyses. All
155 chemical determinations were performed in duplicate with 3 measurements for each
156 replication (n=6).

157 **2.3.1. DPPH activity**

158 The 1,1-Diphenyl-2-Picryl-Hydrazyl (DPPH) activity was measured following the method
159 proposed by Nicklisch and Waite (2014), with the modifications described by Garcia-
160 Vaquero, O'Doherty, Tiwari, Sweeney, and Rajauria (2019). Pepper extracts and ascorbic
161 acid were assayed at 1 mg per mL of working solution (0.1 M citrate phosphate buffer with
162 0.3 % of Triton X-100). The reaction was performed in a Greiner 96 flat-bottomed microplate
163 by adding 10 µL of a 2 mM DPPH solution in methanol to each well. The percentage of
164 DPPH inhibition per mg of extract was calculated by subtracting the absorbance readings of
165 each well at 515 nm prior to DPPH solution addition and at 30 min after DPPH solution
166 addition.

167 **2.3.2. FRAP activity**

168 The ferric reducing antioxidant power (FRAP) was determined using the method described
169 by Benzie and Strain (1996) with the modifications as described by Garcia-Vaquero et al.
170 (2019). Briefly, pepper extracts were assayed against trolox standards in a working solution
171 containing 10:1:1:1.4 of acetate buffer (300 mM, pH 3.6), ferric chloride (20 mM in Milli-Q
172 water), 2,4,6-Tripyridyl-s-Triazine (TPTZ) (10 mM in 40 mM HCl) and Milli-Q water. The
173 reaction was performed in 96 well plates (Greiner Bio-one, Germany) and incubated at 37 °C
174 for 30 min. The absorbance of the reaction was measured at 593 nm using an UV-Vis

175 spectrophotometer (Epoch™ 2, Biotek, VT, USA). FRAP values were expressed as mM
176 trolox equivalents (TE) per 100 g sample.

177 **2.3.3. Total phenolic content**

178 The total phenolic content (TPC) of the pepper extracts was determined according to the
179 method described by Ganesan, Kumar, and Bhaskar (2008) with slight modifications. Briefly,
180 samples at appropriate dilutions were assayed together with gallic acid as standard. 2 mL of a
181 Na₂CO₃ solution (2 %, w/v) were added to 100 µL of the tested extracts. The solutions were
182 mixed with 100 µL of Folin-Ciocalteu phenol reagent (0.5 M) and allowed to stand for 30
183 min in dark conditions. The absorbance of the reaction was measured at 720 nm using an
184 UV-Vis spectrophotometer (Epoch™ 2, Biotek, VT, USA). The total phenolic content (TPC)
185 of the samples was expressed as mg gallic acid equivalents (GAE)/ 100 g sample.

186 **2.4. Spectra acquisition**

187 **2.4.1. NIR MEMS spectrophotometer**

188 Ground peppercorn spectra were acquired using an NIR-MEMS spectrophotometer (NIROne,
189 Spectral Engines Oy, Finland) in the range of 1350 – 1650 nm at 2 nm intervals. The
190 miniaturised NIR-MEMS spectrophotometer consisted of a single element InGaAs detector, a
191 Fabry-Perot interferometer, two tungsten vacuum lamps and an USB interface to a laptop.
192 Black reference (*I_b*) was recorded after turning off the lamp, while the white reference (*I_w*)
193 was recorded using a Thorlab white reference target SM05CP2C (Thorlabs GmbH, Germany)
194 and setting the lamp power to 100%. Samples spectra (*I_s*) were acquired and reflectance
195 calculated according to $R = (I_s - I_b)/(I_w - I_b)$.

196 **2.4.2. Vis-NIR Hyperspectral imaging systems**

197 Hyperspectral images of ground peppercorn were obtained using two line scanning
198 hyperspectral imaging systems (DV Optics, Padova, Italy), one in the visible-near infrared
199 (Vis-NIR) range of 400 - 1000 nm with a spectral resolution of 5 nm and the other in the near

200 infrared (NIR) range of 880 - 1720 nm with a spectral resolution of 7 nm. The Vis-NIR HSI
201 system consisted of a CCD camera (580×580 pixels; Basler, Ahrensburg, Germany), a
202 spectrograph (Spectral Imaging Ltd., Oulu, Finland), cylindrical light diffuser and moving
203 base. The NIR-HSI system consisted of an InGaAs camera (320×240 pixels; Sensors
204 Unlimited, Inc., Princeton, NJ, USA), a spectrograph (Spectral Imaging Ltd., Oulu, Finland),
205 five halogen lamps (3×50 W and 2×20 W), a cylindrical light diffuser, moving base and a
206 computer (Hernández-Hierro et al., 2014). The speed of the moving base was set at 3 mm/s
207 (spatial resolution 0.28×0.28 mm pixel size) and 20 mm/s (spatial resolution 0.3×0.3 mm
208 pixel size) for the Vis-NIR and NIR systems respectively. After scanning 50 lines of black
209 reference and 50 lines of a white tile (reflectance > 93%) with a known reflectance (R_w) the
210 signal from the sample was converted and stored as reflectance $R = R_w (I_s - I_b)/(I_w - I_b)$
211 (Achata, Esquerre, O'Donnell, & Gowen, 2015).

212 Hyperspectral imaging of all samples was carried out at room temperature (~20 °C).
213 Acquired 3-D data hypercubes were saved in ENVI formatted files and imported into
214 MATLAB (The MathWorks Inc., Natick, MA, USA) for further spectral data pre-processing
215 and data analysis, using in-house developed functions and scripts. The spectra obtained from
216 both HSI systems were trimmed to spectral ranges of 450 - 960 nm and 957 - 1664 nm to
217 remove noise at both ends of the spectra. Hypercubes were unfolded by rearranging the three-
218 dimensional hypercubes (X, Y, l) into a two-dimensional matrix (X × Y,) to facilitate
219 algorithm development. Regions of interest (ROI) were carefully selected from each sample
220 to avoid edge effects detected following analysis of PCA scores maps. Mean spectra of each
221 sample were calculated from the selected ROI and used for model development.

222 **2.5. Principal component analysis**

223 PCA of standard normal variate (SNV) pretreated spectral datasets was carried out to
224 investigate the relationships between the peppercorn samples and spectra acquired using the 3

225 spectroscopy systems, and also to identify potential outliers using the T^2 statistic. A sample
226 was considered as an outlier if the T^2 value was $> T^2_{crit} = A \times F_{(0.05, A, n - A)} \times (n - 1) / (n - A)$, where A
227 is the number of significant components, n is the number of spectra in the dataset and $F_{(0.05, A, n - A)}$
228 $- A)$ is the F statistic (with $\alpha = 0.05$, A and $n - A$ degrees of freedom)

229

230 **2.6. Development of prediction models**

231 PLS regression models to predict moisture, antioxidant capacity and total phenolic content of
232 samples were developed using spectral data, spectral pre-treatments and the ensemble Monte
233 Carlo variable selection (EMCVS) method. SNV, median scaled (MS), Savitzky-Golay 7
234 points second order polynomial first derivative (FD), Savitzky-Golay 7 points second order
235 polynomial second derivative (SD), Savitzky-Golay 11 points fourth order polynomial third
236 derivative (TD), linear detrending second-order polynomial (LD), asymmetric least squares
237 (AsLs) and all combinations of any two spectral pre-treatments were tested. The EMCVS
238 method was employed to select the bands that produce the most stable regression coefficients
239 (Esquerre, Gowen, O'Gorman, Downey, & O'Donnell, 2017). The spectral datasets were split
240 randomly into calibration and validation datasets. The number of latent variables in the PLS
241 model were selected using the root mean square of 10-fold cross validation and a jaggedness
242 of the regression vector to avoid overfitting (Gowen, Downey, Esquerre, & O'Donnell, 2011).

243 The performance of the regression models was assessed using the root mean square error
244 (RMSE), the coefficient of determination (R^2), the ratio of standard deviation of the reference
245 data and the RMSE (RPD) for cross-validation and validation sets. The best model was
246 selected based on the number of latent variables, selected wavebands and the geometric mean
247 of the RPD values from calibration ($n = 123$) and validation ($n = 41$) sets. The performance
248 of the prediction models based on RPD values for complex matrices can be classified as
249 excellent (RPD > 4.1), very good (RPD 3.5 – 4.0), good (RPD 3.0 – 3.4), fair (RPD 2.5 – 2.9)

250 and poor (RPD 2.0 – 2.4) (Williams, 2014). It is not recommended to use a prediction model
251 when the RPD values are in the range 0.0 - 1.9.

252

253 3. Results and discussion

254 3.1. Ground peppercorn moisture, antioxidant capacity and TPC

255 The moisture, antioxidant capacity (DPPH and FRAP) and TPC of control black, white, green
256 and pink peppercorn samples are summarised in Table 1. Pink peppercorn samples had higher
257 TPC and antioxidant activities than the other peppercorn types. White peppercorn samples
258 had the lowest levels of all analysed parameters. The high TPC values in pink peppercorns
259 (*Schinus terebinthifolius*) may be due to interspecies variation with respect to *Piper nigrum*
260 L. (black, white and green peppercorns). Similar variations were reported by Shan, Cai, Sun,
261 and Corke (2005) with TPC values ranging from 0.30-0.78 g GAE per 100 g DW in black,
262 white and green peppercorns. Differences in TPC values between black and white
263 peppercorns were also investigated by Agbor, Vinson, Oben, and Ngogang (2006), with a
264 higher concentration of TPC in black compared to white peppercorns reported.

265 3.2. Ground peppercorn spectra

266 Figure 1 shows the mean spectra of the control samples acquired using the three spectroscopy
267 systems i.e. NIR-MEMS, Vis-NIR HSI and NIR HSI. The NIR-MEMS spectra of the control
268 samples were similar. A broad absorption band may be observed around 1468 nm (Figure 1a)
269 which can be attributed to the first overtone of the H-OH bond (Rodriguez-Saona, Ayvaz, &
270 Wehling, 2017; Segtnan, Sasic, Isaksson, & Ozaki, 2001). Large variations may be observed
271 between the Vis-NIR HSI spectra of the control samples (Figure 1b). The main difference
272 between the spectra is the sharp absorption band around 665 nm in the green peppercorn
273 spectra which is related to chlorophyll content (Seifert & Zude-Sasse, 2016). The NIR-HSI
274 spectra of the control samples have similar profiles. In addition to a broad band at 1468 nm,

275 an absorption band around 1202 nm may observed which can be attributed to the 2nd overtone
276 of C-H bond stretching (Figure 1c). Shoulders are also observed around 1272 nm (water-
277 protein interaction), 1363 nm and 1580 nm in the NIR-HSI spectra.

278 3.3. Principal component analysis

279 PCA of SNV pretreated spectra (n= 164) of the ground peppercorn samples identified three
280 samples as outliers using the T^2 statistic. The first three PCs of the remaining ground
281 peppercorn SNV treated spectra (n=161) from the NIR-MEMS, Vis-NIR HSI and NIR HSI
282 systems are shown in Figure 2. Good separation of the four types of peppercorn was observed
283 in the PC score plots for the 3 spectroscopy systems (Figure 2). Ninety two % of the variance
284 in the NIR-MEMS data was explained by the first two principal components PC1 (73%) and
285 PC2(19%). PC1 loadings were largely influenced by the absorption bands attributed to
286 weakly (1410 nm) and strongly (1456 nm) H-bonded water (Segtnan et al., 2001). Whereas
287 98% of variance in the Vis-NIR HSI data were explained by the first two principal
288 components PC1 (54%) and PC2 (44%). PC1 loadings were mainly influenced by absorption
289 bands at 650 nm which may be attributed to chlorophyll (Seifert & Zude-Sasse, 2016). In the
290 NIR-HSI spectra PC1 explained 93.2% of the variance with PC1 loadings mainly influenced
291 by the absorption bands at 1216, 1342, 1412 and 1643 nm which may be attributed to the 2nd
292 overtone of C-H bond stretching, the combination of -CH₂, first overtone of -OH stretching in
293 water and first overtone of aromatic -CH respectively (Kumagai et al., 2003; Rodriguez-
294 Saona et al., 2017; Šašić & Ozaki, 2000).

295

296 3.4. Prediction models for moisture, antioxidant capacity and TPC

297 Table 2 shows the best performing models developed using the NIR-MEMS, Vis-NIR HSI
298 and NIR HSI systems to predict moisture, DPPH, FRAP and TPC. These models were built
299 using 120 randomly selected samples and validated using the remaining 41 samples.

300 The best prediction models developed using the NIR-MEMS performed very well for TPC
301 (RPD 3.5-3.7), fairly for FRAP (RPD 2.5), poorly for moisture (RPD 2.3-2.5) and were not
302 suitable for DPPH (RPD 1.8-2.1) prediction. The performance of the best prediction models
303 developed using the Vis-NIR HSI and NIR HSI spectral ranges were similar for DPPH,
304 FRAP and TPC yielding good (RPD 2.9-3.1), fair (RPD 2.8-2.9) and very good (RPD 3.8-
305 4.1) predictions respectively. The best moisture content prediction model developed using the
306 NIR HSI spectra yielded very good (RPD > 3.5) predictions, while the best model developed
307 using the Vis-NIR HSI spectra yielded poor moisture content predictions (RPD 2.3-2.4). The
308 very good performance of the models developed using the validation sets (Table 2)
309 demonstrated the potential of NIR-MEMS and Vis-NIR/NIR HSI to predict the moisture
310 content, antioxidant capacity and total phenolic content of peppercorns. Both technologies
311 can be used for in-line control of multiple analytes in peppercorn processing.

312 Figure 3 shows the selected bands for the best prediction models developed using the NIR
313 HSI spectral range. The selected bands in the range 978, 1013 – 1160, 1083 - 1174, 1265 -
314 1286, 1342, 1405 - 1450, 1461 - 1475 and 1538 - 1664 nm may be attributed to the second
315 overtone O-H stretching, the second overtone of C-H stretching in -CH₃ groups, the
316 combination of -CH₂, protein-water interaction, the first overtone of C-H stretching and C-H
317 bending combination, first overtone O-H stretching of weak bonded water, first overtone O-H
318 stretching of strong bonded water and first overtone of aromatic -CH respectively (Kumagai
319 et al., 2003; Rodriguez-Saona et al., 2017; Šašić & Ozaki, 2000).

320 Due to the larger spectral range of the NIR HSI system, better prediction models were
321 developed compared to the NIR-MEMS systems. However the prediction models developed
322 using the NIR-MEMS spectra performed very well for TPC and fairly for FRAP. Sensor
323 fusion of multiple complementary NIR MEMS systems based on FPIs could be employed to

324 extend the total spectral range measured for model development and improve prediction
325 performance.

326

327 **4. Conclusions**

328 This study demonstrated the potential of an NIR MEMS spectrophotometer and Vis-NIR/NIR
329 hyperspectral imaging systems to predict moisture content, antioxidant capacity and total
330 phenolic content properties of ground peppercorns. The potential of the NIR-MEMS
331 spectrophotometer for food applications was demonstrated through prediction models
332 developed for FRAP (RPD > 2.4) and total phenolic content (RPD > 3.6) of ground
333 peppercorns. Both HSI systems investigated were demonstrated to be suitable for use as rapid
334 process analytical tools for evaluation of antioxidant capacity (DPPH RPD > 3.0, FRAP RPD
335 >2.9) and TPC (RPD > 3.8) of ground peppercorns. The NIR HSI system has the additional
336 benefit of very good moisture content prediction. Sensor fusion of multiple complementary
337 NIR MEMS systems based on FPIs could be employed to extend the spectral range for model
338 development and improve prediction performance. Band selection and spectral pre-treatments
339 were key for robust prediction model development. The three spectroscopy systems
340 investigated may be employed as in-line PAT tools to provide improved control and
341 understanding in peppercorn processing.

342

343 Funding: This research did not receive any specific grant from funding agencies in the public,
344 commercial, or not-for-profit sectors.

345 Declaration of competing interest:

346 The authors declare no conflict of interest.

347 Table 1. Moisture, DPPH, FRAP and TPC of control ground peppercorn samples.

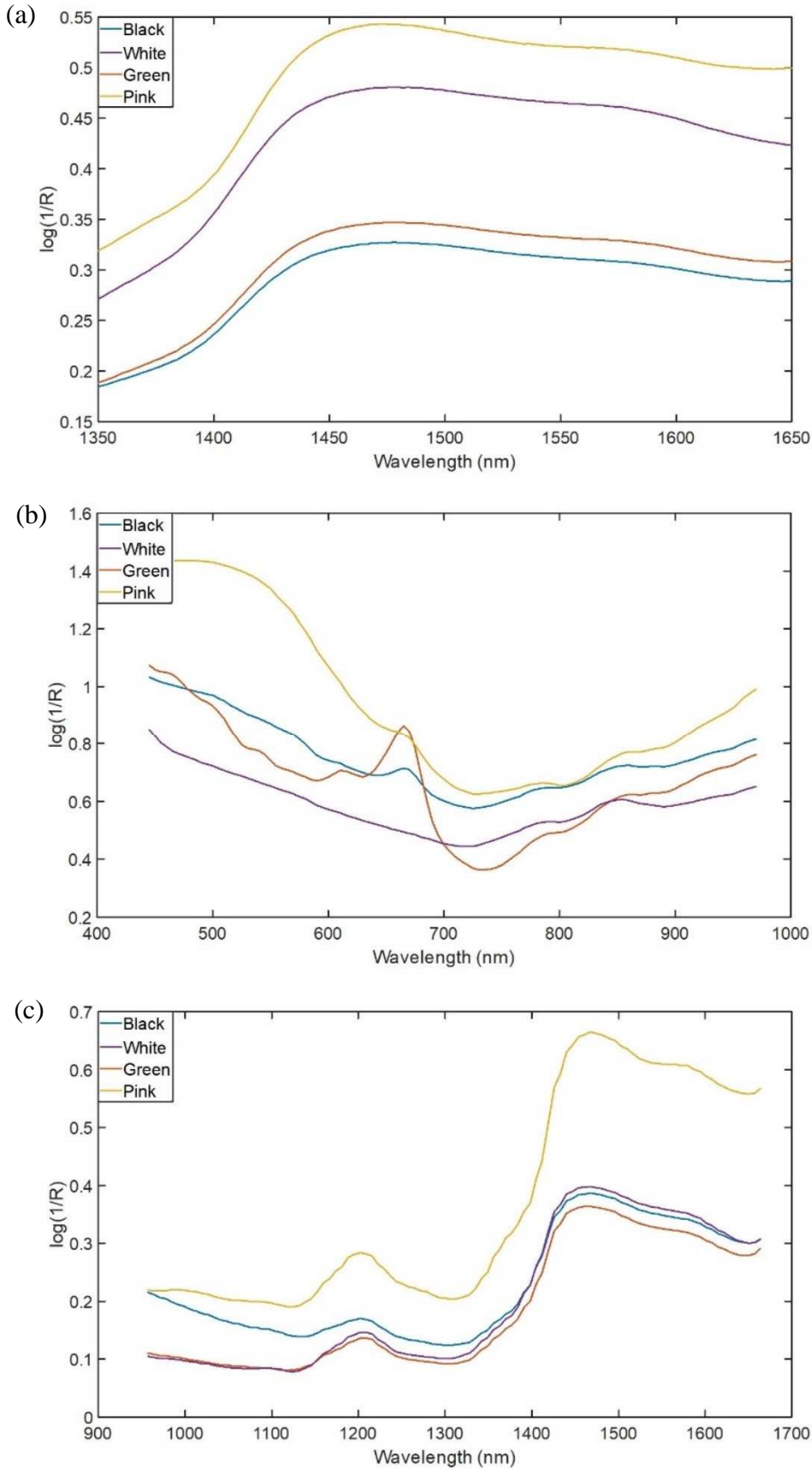
Peppercorn type	Moisture (g/100 g sample)*	DPPH (%)*	FRAP (mM TE/100 g sample)*	TPC (mg GAE/100 g sample)*
Black	10.9 ± 0.2	83.0 ± 2.1	1005 ± 87	633 ± 35
White	11.1 ± 0.2	57.0 ± 3.9	279 ± 4	156 ± 6
Green	8.5 ± 0.1	90.8 ± 0.8	3089 ± 512	832 ± 52
Pink	13.2 ± 0.2	98.9 ± 1.1	8336 ± 164	2761 ± 193

348 * Values represents mean ± standard error (n = 2)

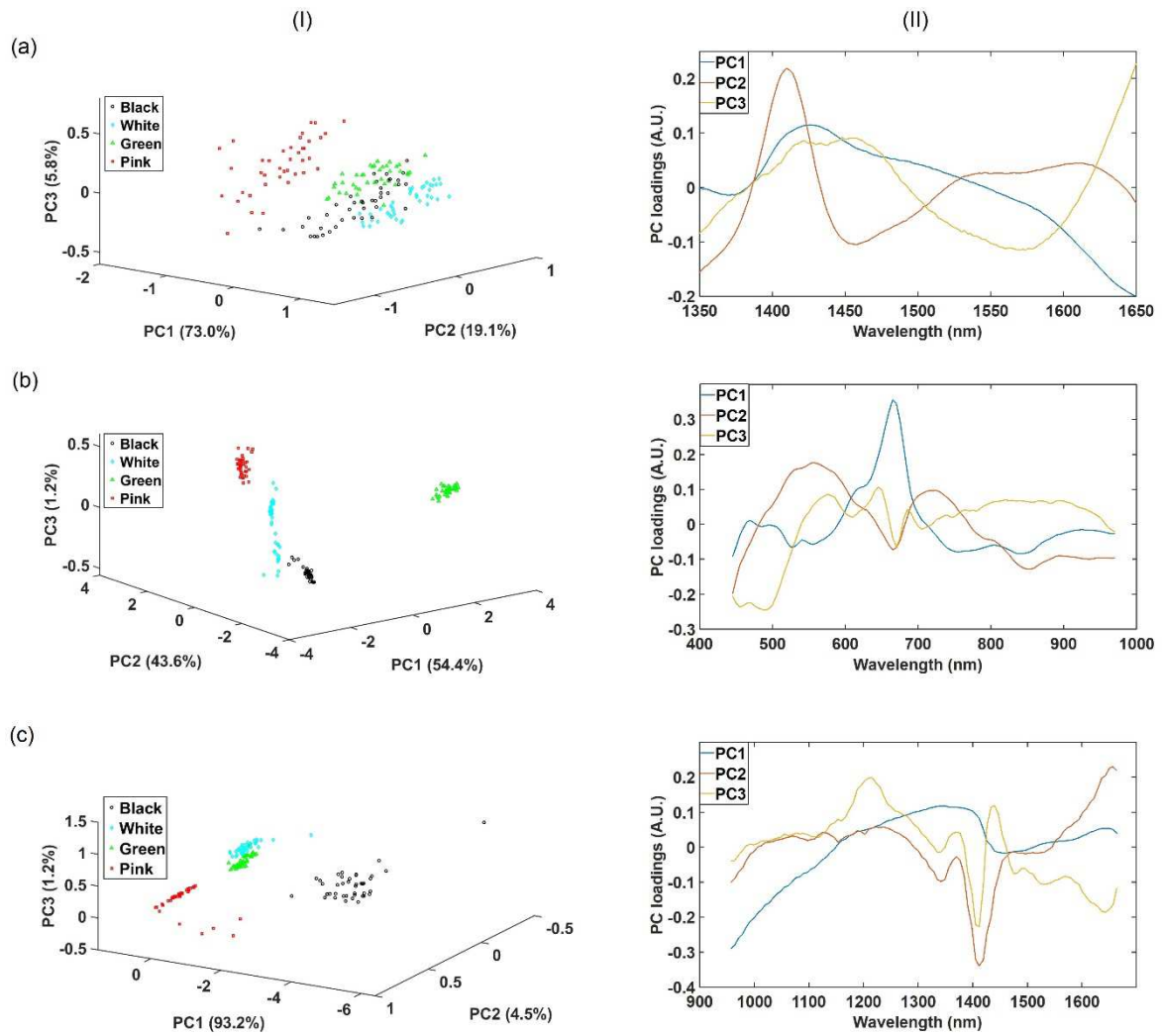
349 Table 2. Performance of prediction models developed using MEMS NIR, Vis – NIR HSI and NIR HSI systems to predict moisture (g/100 g
 350 sample), DPPH (%), FRAP (mM TE/100 g sample) and TPC (mg GAE/100 g sample) of ground peppercorns.

	System	R/log(1/R)	Pre-treatment	N Bands	N LV	Cross Validation			Validation		
						RMSECV	RPDCV	R ² CV	RMSEP	RPDP	R ² P
Moisture	NIR-MEMS	R	MS+AsLS	19	5	1.0	2.3	0.80	1.1	2.5	0.84
	Vis-NIR HSI	log(1/R)	SNV+2Der	9	6	1.0	2.4	0.83	1.2	2.3	0.83
	NIR-HSI	log(1/R)	-	25	7	0.7	3.5	0.92	0.8	3.7	0.93
DPPH	NIR-MEMS	log(1/R)	MS+2Der	10	3	10.7	2.2	0.79	13.9	1.7	0.64
	Vis-NIR HSI	R	MS+1Der	9	3	7.6	3.1	0.90	7.9	3.0	0.89
	NIR-HSI	R	1Der	16	4	8.0	2.9	0.88	7.9	3.0	0.89
FRAP	NIR-MEMS	R	SNV+LD	36	6	1452	2.5	0.84	1924	2.5	0.86
	Vis-NIR HSI	R	2Der+SNV	6	4	1232	2.9	0.88	1651	2.8	0.88
	NIR-HSI	log(1/R)	LD+2Der	31	5	1281	2.8	0.87	1670	2.9	0.90
TPC	NIR-MEMS	log(1/R)	AsLs	30	6	340	3.5	0.92	395	3.7	0.93
	Vis-NIR HSI	log(1/R)	LD+1Der	5	3	317	3.8	0.93	357	4.1	0.94
	NIR-HSI	log(1/R)	LD	21	5	320	3.8	0.93	384	4.0	0.94

351 The best models for each analyte are marked in bold. R: reflectance, N Bands: number of bands included in the model, N LV: number of latent
 352 variables used in the model, RMSE: root mean square error in cross validation, RPD: the ratio of standard deviation of the reference data of
 353 calibration set and the RMSECV, R²: square of the coefficient of correlation, CV: crossvalidation, P: validation set, MS: median centred, AsLs:
 354 asymmetric least squares, SNV: standard normal variate, 2Der: seconderivative, 1Der: first derivative, LD:linear detrending.

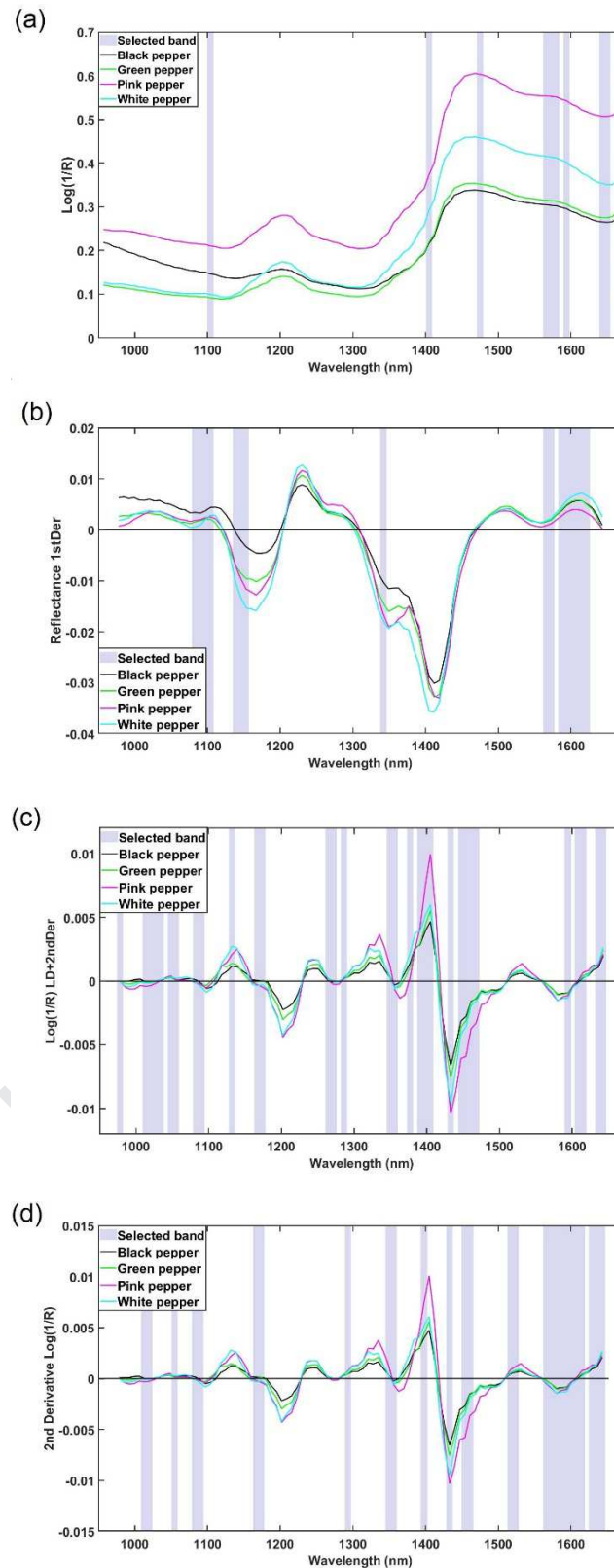


355 Figure 1. Mean spectra of control samples of black, white, green and pink ground peppercorn
 356 samples acquired using (a) NIR-MEMS, (b) Vis-NIR HSI and (c) NIR HSI systems



357 Figure 2. Principal component analysis scores (I) and loadings (II) of the three first principal
 358 components (a) NIR-MEMS (b) Vis-NIR HSI (c) NIR-HSI SNV treated spectra of ground
 359 peppercorn samples

360



361 Figure 3. Mean ground peppercorn NIR-HSI pretreated spectra and selected bands for (a)
 362 moisture, (b) DPPH, (c) FRAP and (d) TPC prediction.

363

364 **References**

- 365 Achata, E. M., Esquerre, C., O'Donnell, C. P., & Gowen, A. A. (2015). A study on the
366 application of near infrared hyperspectral chemical imaging for monitoring moisture
367 content and water activity in low moisture systems. *Molecules (Basel, Switzerland)*,
368 *20*(2), 2611-2621. doi: <https://doi.org/10.3390/molecules20022611>
- 369 Achata, E. M., Inguglia, E. S., Esquerre, C., Tiwari, B. K., & O'Donnell, C. P. (2019).
370 Evaluation of Vis-NIR hyperspectral imaging as a process analytical tool to classify
371 brined pork samples and predict brining salt concentration. *Journal of Food*
372 *Engineering*, *246*, 134-140. doi: <https://doi.org/10.1016/j.jfoodeng.2018.10.022>
- 373 Benzie, I. F. F., & Strain, J. J. (1996). The Ferric Reducing Ability of Plasma (FRAP) as a
374 Measure of "Antioxidant Power": The FRAP Assay. *Analytical Biochemistry*, *239*(1),
375 70-76. doi: <https://doi.org/10.1006/abio.1996.0292>
- 376 Charoux, C. M. G., Free, L., Hinds, L. M., Vijayaraghavan, R. K., Daniels, S., O'Donnell, C.
377 P., & Tiwari, B. K. (2020). Effect of non-thermal plasma technology on microbial
378 inactivation and total phenolic content of a model liquid food system and black
379 pepper grains. *LWT*, *118*, 108716. doi: <https://doi.org/10.1016/j.lwt.2019.108716>
- 380 Esquerre, C., Gowen, A. A., Burger, J., Downey, G., & O'Donnell, C. P. (2012). Suppressing
381 sample morphology effects in near infrared spectral imaging using chemometric data
382 pre-treatments. *Chemometrics and Intelligent Laboratory Systems*, *117*(0), 129-137.
383 doi: <https://doi.org/10.1016/j.chemolab.2012.02.006>
- 384 Esquerre, C., Gowen, A. A., O'Gorman, A., Downey, G., & O'Donnell, C. P. (2017).
385 Evaluation of ensemble Monte Carlo variable selection for identification of metabolite
386 markers on NMR data. *Analytica Chimica Acta*, *964*, 45-54. doi:
387 <https://doi.org/10.1016/j.aca.2017.01.027>
- 388 Friedman, M., Levin, C. E., Lee, S.-U., Lee, J.-S., Ohnisi-Kameyama, M., & Kozukue, N.
389 (2008). Analysis by HPLC and LC/MS of Pungent Piperamides in Commercial Black,
390 White, Green, and Red Whole and Ground Peppercorns. *Journal of Agricultural and*
391 *Food Chemistry*, *56*(9), 3028-3036. doi: <https://doi.org/10.1021/jf703711z>
- 392 Ganesan, P., Kumar, C. S., & Bhaskar, N. (2008). Antioxidant properties of methanol extract
393 and its solvent fractions obtained from selected Indian red seaweeds. *Bioresource*
394 *Technology*, *99*(8), 2717-2723. doi: <https://doi.org/10.1016/j.biortech.2007.07.005>
- 395 Garcia-Vaquero, M., O'Doherty, J. V., Tiwari, B. K., Sweeney, T., & Rajauria, G. (2019).
396 Enhancing the Extraction of Polysaccharides and Antioxidants from Macroalgae
397 Using Sequential Hydrothermal-Assisted Extraction Followed by Ultrasound and
398 Thermal Technologies. *Marine Drugs*, *17*(8), 457. doi:
399 <https://doi.org/10.3390/md17080457>
- 400 Gomes, R. B. d. A., de Souza, E. S., Gerhardt Barraqui, N. S., Tosta, C. L., Nunes, A. P. F.,
401 Schuenck, R. P., . . . Kuster, R. M. (2020). Residues from the Brazilian pepper tree
402 (*Schinus terebinthifolia* Raddi) processing industry: Chemical profile and
403 antimicrobial activity of extracts against hospital bacteria. *Industrial Crops and*
404 *Products*, *143*, 111430. doi: <https://doi.org/10.1016/j.indcrop.2019.05.079>
- 405 Gowen, A. A., Downey, G., Esquerre, C., & O'Donnell, C. P. (2011). Preventing over-fitting
406 in PLS calibration models of near-infrared (NIR) spectroscopy data using regression
407 coefficients. *Journal of Chemometrics*, *25*(7), 375-381. doi:
408 <https://doi.org/10.1002/cem.1349>
- 409 Gowen, A. A., O'Donnell, C. P., Cullen, P. J., Downey, G., & Frias, J. M. (2007).
410 Hyperspectral imaging - an emerging process analytical tool for food quality and
411 safety control. *Trends in Food Science and Technology*, *18*(12), 590-598. doi:
412 <https://doi.org/10.1016/j.tifs.2007.06.001>

- 413 Hernández-Hierro, J. M., Esquerre, C., Valverde, J., Villacreces, S., Reilly, K., Gaffney, M., .
414 . . Downey, G. (2014). Preliminary study on the use of near infrared hyperspectral
415 imaging for quantitation and localisation of total glucosinolates in freeze-dried
416 broccoli. *Journal of Food Engineering*, *126*, 107-112. doi:
417 <https://doi.org/10.1016/j.jfoodeng.2013.11.005>
- 418 Kumagai, M., Suyama, H., Sato, T., Amano, T., Kikuchi, R., & Ogawa, N. (2003). Chemical
419 Meaning of Near Infrared Spectra from a Portable Near Infrared Spectrometer for
420 Various Plastic Wastes. *International Journal of the Society of Materials Engineering
421 for Resources*, *11*(1), 5-9. doi: <https://doi.org/10.5188/ijsmer.11.5>
- 422 Lapcharoensuk, R., Chalachai, S., Sinjaru, S., Singsriand, P., Hongwiangjan, J., &
423 Yaemphochai, N. (2019). *Quantitative detection of pepper powder adulterated with
424 rice powder using Fourier-transform near infrared spectroscopy*. Paper presented at
425 the IOP Conference Series: Earth and Environmental Science.
- 426 Meghwal, M., & Goswami, T. K. (2013). Piper nigrum and Piperine: An Update.
427 *Phytotherapy Research*, *27*(8), 1121-1130. doi: <https://doi.org/10.1002/ptr.4972>
- 428 Mendelson, Y. (2012). Chapter 10 - Biomedical Sensors. In J. D. Enderle & J. D. Bronzino
429 (Eds.), *Introduction to Biomedical Engineering (Third Edition)* (pp. 609-666).
430 Boston: Academic Press.
- 431 Misra, N. N., Patil, S., Moiseev, T., Bourke, P., Mosnier, J. P., Keener, K. M., & Cullen, P. J.
432 (2014). In-package atmospheric pressure cold plasma treatment of strawberries.
433 *Journal of Food Engineering*, *125*, 131-138. doi:
434 <https://doi.org/10.1016/j.jfoodeng.2013.10.023>
- 435 Montenegro, J., Ruan, R., Ma, H., & Chen, P. (2002). Inactivation of E. coli O157:H7 Using
436 a Pulsed Nonthermal Plasma System. *Journal of Food Science*, *67*(2), 646-648. doi:
437 <https://doi.org/10.1111/j.1365-2621.2002.tb10653.x>
- 438 Mujica, L. E., Rodellar, J., Fernández, A., & Güemes, A. (2010). Q-statistic and T2-statistic
439 PCA-based measures for damage assessment in structures. *Structural Health
440 Monitoring*, *10*(5), 539-553. doi: <https://doi.org/10.1177/1475921710388972>
- 441 Nicklisch, S. C. T., & Waite, J. H. (2014). Optimized DPPH assay in a detergent-based buffer
442 system for measuring antioxidant activity of proteins. *MethodsX*, *1*, 233-238. doi:
443 <https://doi.org/10.1016/j.mex.2014.10.004>
- 444 Nikolić, M., Stojković, D., Glamočlija, J., Ćirić, A., Marković, T., Smiljković, M., &
445 Soković, M. (2015). Could essential oils of green and black pepper be used as food
446 preservatives? *Journal of food science and technology*, *52*(10), 6565-6573. doi:
447 <https://doi.org/10.1007/s13197-015-1792-5>
- 448 O'Donnell, C. P., Fagan, C., & Cullen, P. J. (2014). *Process Analytical Technology for the
449 Food Industry*.
- 450 Orrillo, I., Cruz-Tirado, J. P., Cardenas, A., Oruna, M., Carnero, A., Barbin, D. F., & Siche,
451 R. (2019). Hyperspectral imaging as a powerful tool for identification of papaya seeds
452 in black pepper. *Food Control*, *101*, 45-52. doi:
453 <https://doi.org/10.1016/j.foodcont.2019.02.036>
- 454 Parashar, A., Shah, A., Packirisamy, M., & Sivakumar, N. (2007). Three Cavity Tunable
455 MEMS Fabry Perot Interferometer. *Sensors*, *7*(12), 3071-3083. doi:
456 <https://doi.org/10.3390/s7123071>
- 457 Plessi, M., Bertelli, D., & Miglietta, F. (2002). Effect of Microwaves on Volatile Compounds
458 in White and Black Pepper. *LWT - Food Science and Technology*, *35*(3), 260-264.
459 doi: <https://doi.org/10.1006/fstl.2001.0853>
- 460 Pu, Y.-Y., O'Donnell, C., Tobin, J. T., & O'Shea, N. (2020). Review of near-infrared
461 spectroscopy as a process analytical technology for real-time product monitoring in

- 462 dairy processing. *International Dairy Journal*, 103, 104623. doi:
463 <https://doi.org/10.1016/j.idairyj.2019.104623>
- 464 Rodriguez-Saona, L. E., & Aykas, D. P. (2019). New Approaches for Rapid Tomato Quality
465 Control. In S. Porretta (Ed.), *Tomato Chemistry, Industrial Processing and Product*
466 *Development*.
- 467 Rodriguez-Saona, L. E., Ayvaz, H., & Wehling, R. L. (2017). Infrared and Raman
468 Spectroscopy. In S. Nielsen (Ed.), *Food Analysis* (pp. 107-127): Springer.
- 469 Šašić, S., & Ozaki, Y. (2000). Band Assignment of Near-Infrared Spectra of Milk by Use of
470 Partial Least-Squares Regression. *Applied Spectroscopy*, 54(9), 1327-1338.
- 471 Schiffmann, R. F. (2014). Microwave and Dielectric Drying. In A. S. Mujumdar (Ed.),
472 *Handbook of Industrial Drying*: CRC Press.
- 473 Schulz, H., Baranska, M., Quilitzsch, R., Schütze, W., & Lösing, G. (2005). Characterization
474 of Peppercorn, Pepper Oil, and Pepper Oleoresin by Vibrational Spectroscopy
475 Methods. *Journal of Agricultural and Food Chemistry*, 53(9), 3358-3363. doi:
476 <https://doi.org/10.1021/jf048137m>
- 477 Segtnan, V. H., Sasic, S., Isaksson, T., & Ozaki, Y. (2001). Studies on the Structure of Water
478 Using Two-Dimensional Near-Infrared Correlation Spectroscopy and Principal
479 Component Analysis. *Analytical Chemistry*, 73(13), 3153-3161. doi:
480 <http://dx.doi.org/10.1021/ac010102n>
- 481 Seifert, B., & Zude-Sasse, M. (2016). High hydrostatic pressure effects on spectral-optical
482 variables of the chlorophyll pool in climacteric fruit. *LWT*, 73, 303-310. doi:
483 <https://doi.org/10.1016/j.lwt.2016.06.011>
- 484 Shityakov, S., Bigdelian, E., Hussein, A. A., Hussain, M. B., Tripathi, Y. C., Khan, M. U., &
485 Shariati, M. A. (2019). Phytochemical and pharmacological attributes of piperine: A
486 bioactive ingredient of black pepper. *European Journal of Medicinal Chemistry*, 176,
487 149-161. doi: <https://doi.org/10.1016/j.ejmech.2019.04.002>
- 488 Wang, Y.-C., Shyu, L.-H., & Chang, C.-P. (2010). The Comparison of Environmental Effects
489 on Michelson and Fabry-Perot Interferometers Utilized for the Displacement
490 Measurement. *Sensors*, 10(4), 2577-2586. doi: <https://doi.org/10.3390/s100402577>
- 491 Wilde, A. S., Haughey, S. A., Galvin-King, P., & Elliott, C. T. (2019). The feasibility of
492 applying NIR and FT-IR fingerprinting to detect adulteration in black pepper. *Food*
493 *Control*, 100, 1-7. doi: <https://doi.org/10.1016/j.foodcont.2018.12.039>
- 494 Williams, P. (2014). The RPD Statistic: A Tutorial Note. *NIR news*, 25(1), 22-26. doi:
495 <https://doi.org/10.1255/nirn.1419>
- 496 Yan, H., & Siesler, H. W. (2018). Identification Performance of Different Types of Handheld
497 Near-Infrared (NIR) Spectrometers for the Recycling of Polymer Commodities.
498 *Applied Spectroscopy*, 72(9), 1362-1370. doi:
499 <https://doi.org/10.1177/0003702818777260>
- 500 Zimmerleiter, R., Kager, J., Nikzad-Langerodi, R., Berezinskiy, V., Westad, F., Herwig, C.,
501 & Brandstetter, M. (2019). Probeless non-invasive near-infrared spectroscopic
502 bioprocess monitoring using microspectrometer technology. *Analytical and*
503 *Bioanalytical Chemistry*. doi: <https://doi.org/10.1007/s00216-019-02227-w>

504

Highlights

- NIR MEMS and Vis/NIR hyperspectral imaging predict antioxidant capacity of peppercorns.
- NIR MEMS and Vis/NIR hyperspectral imaging predict total phenolic content of peppercorns.
- Band selection and spectral pre-treatments were key for robust prediction model development.
- NIR MEMS and hyperspectral imaging may be employed as in-line PAT tools in peppercorn processing.

Conflicts of Interest Statement

Manuscript title: Use of an NIR MEMS spectrophotometer and visible/NIR hyperspectral imaging systems to

predict quality parameters of treated ground peppercorns

The authors whose names are listed immediately below certify that they have NO affiliations with or involvement in any organization or entity with any financial interest (such as honoraria; educational grants; participation in speakers' bureaus; membership, employment, consultancies, stock ownership, or other equity interest; and expert testimony or patent-licensing arrangements), or non-financial interest (such as personal or professional relationships, affiliations, knowledge or beliefs) in the subject matter or materials discussed in this manuscript.

Author names:






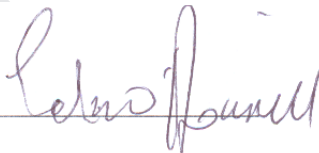
Carlos A. Esquerre
Eva M. Achata
Marco García-Vaquero
Zhihang Zhang
Brijesh Tiwari
Colm P. O'Donnell

The authors whose names are listed immediately below report the following details of affiliation or involvement in an organization or entity with a financial or non-financial interest in the subject matter or materials discussed in this manuscript. Please specify the nature of the conflict on a separate sheet of paper if the space below is inadequate.

Author names:

N/A

This statement is signed by all the authors to indicate agreement that the above information is true and correct (a photocopy of this form may be used if there are more than 10 authors):

Author's name (typed)	Author's signature	Date
Carlos A. Esquerre		11/03/2020
Eva M. Achata		11/03/2020
Marco García-Vaquero		11/03/2020
Zhihang Zhang		11/03/2020
Brijesh Tiwari		11/03/2020
Colm P. O'Donnell		11/03/2020